Article

Not peer-reviewed version

Powders Synthesized from Calcium Chloride and Mixed-Anionic Solution Containing Orthophosphate and Carbonate Ions

Tatiana V. Safronova *, Hieu Minh Ngoc Le, Tatiana B. Shatalova, Albina M. Murashko, Tatiana V. Filippova, Egor. A. Motorin, Dmitry M. Tsymbarenko, Daniil O. Golubchikov, Olga V. Boytsova, Alexander V. Knotko

Posted Date: 1 September 2025

doi: 10.20944/preprints202508.2229.v1

Keywords: synthesis; mixed anionic solution; hydroxyapatite; brushite; calcite; sylvine; monetite; calcium pyrophosphate; tricalcium phosphate; calcium potassium pyrophosphate; chlorapatite

Article

Powders Synthesized from Calcium Chloride and Mixed-Anionic Solution Containing Orthophosphate and Carbonate Ions

Tatiana V. Safronova [1,2,*], Hieu Minh Ngoc Le [1], Tatiana B. Shatalova [1,2], Albina M. Murashko [2], Tatiana V. Filippova [1], Egor. A. Motorin [2], Dmitry M. Tsymbarenko [1], Daniil O. Golubchikov [2], Olga V. Boytsova [1,2], and Alexander V. Knotko [2]

[1] Department of Chemistry, Lomonosov Moscow State University, Building, 3, Leninskie Gory, 1, 119991 Moscow, Russia

[2] Department of Materials Science, Lomonosov Moscow State University, Building, 73, Leninskie Gory, 1, 119991 Moscow, Russia

* Correspondence: safronovatv@my.msu.ru; Tel.: +7-(916)-3470641

Abstract

Low crystalline hydroxyapatite was synthesized from an aqueous solution of calcium chloride $CaCl_2$ and a mixed-anionic (HPO_4^{2-} и CO_3^{2-}) aqueous solution prepared from potassium hydrophosphate trihydrate K_2HPO_4 $3H_2O$ and potassium carbonate K_2CO_3. The interaction of K_2CO_3 and K_2HPO_4 salts during synthesis from a mixed anionic solution in the reaction zone without additional regulation provided the pH level necessary for the synthesis of hydroxyapatite. For comparison, as references, powders were also synthesized from an aqueous solution of calcium chloride $CaCl_2$ and from aqueous solutions of either potassium hydrophosphate K_2HPO_4 or potassium carbonate K_2CO_3. The phase composition of the powder synthesized from aqueous solutions of calcium chloride $CaCl_2$ and potassium hydrophosphate K_2HPO_4 included brushite $CaHPO_4{\cdot}2H_2O$. The phase composition of the powder synthesized from aqueous solutions of calcium chloride $CaCl_2$ and potassium carbonate K_2CO_3 included calcite $CaCO_3$. The phase composition of all synthesized powders contained potassium chloride (sylvine) KCl as a reaction by-product. After heat treatment at 1000 °C of the powder containing low crystalline hydroxyapatite and potassium chloride (sylvine) KCl, powder of chlorapatite $Ca_{10}(PO_4)_6Cl_2$ was obtained. After heat treatment of a powder containing brushite $CaHPO_4{\cdot}2H_2O$ and potassium chloride (sylvine) KCl at 800 and 1000 °C, a powder with the phase composition including β-calcium pyrophosphate β-$Ca_2P_2O_7$, β-calcium orthophosphate β-$Ca_3(PO_4)_2$ and potassium-calcium pyrophosphate $K_2CaP_2O_7$ was obtained. Heat treatment of calcite $CaCO_3$ powder at 800 °C, as expected, led to the formation of calcium oxide CaO. Synthesized powders including biocompatible minerals such as hydroxyapatite, chlorapatite, brushite, monetite, calcium pyrophosphate, calcium potassium pyrophosphate, tricalcium phosphate, calcite can be used for creation of biocompatible inorganic materials or composite materials with a biocompatible polymer matrix. The potassium chloride present in the synthesized powders can act as one of the precursors of biocompatible minerals such as chlorapatite or calcium potassium pyrophosphate; or it can be treated as a removable inorganic porogen.

Keywords: synthesis; mixed anionic solution; hydroxyapatite; brushite; calcite; sylvine; monetite; calcium pyrophosphate; tricalcium phosphate; calcium potassium pyrophosphate; chlorapatite

 doi:10.20944/preprints202508.2229.v1

1. Introduction

Fine powders with a given chemical and phase composition and high uniformity of component distribution are required for creation of inorganic materials or composite materials with unique functional properties [1–3]. The simplest and most obvious is the method of mechanical homogenization of powder mixtures, which is carried out using special equipment, such as a planetary mill [4]. High-temperature solid-phase synthesis from a homogeneous mixture of salts obtained by drying a solution of these salts at subzero temperatures is more difficult for implementation [5]. The maximum level of homogenization is achieved in mixed-anionic compounds, which are produced using high-temperature (synthesis in the solid phase, synthesis by interaction of gas and solid phases, synthesis using pressure) and low-temperature reactions (topochemical, solvothermal synthesis, synthesis in thin films) [6]. Precipitation of hydroxides [7], carbonates or oxalates are also used to obtain homogeneous precursors of oxide powders [8]. Synthesis of inorganic powders consisting of small particles with a high specific surface area and activity via precipitation from solution is the most convenient for implementation [9].

High uniformity of the distribution of components in a powder intended for the production of biocompatible materials can be achieved using synthesis from both mixed-cationic [10] and mixed-anionic solutions, for example, containing $HPO_4^{2-}/P_2O_7^{4-}$ [11], HPO_4^{2-}/CO_3^{2-} [12–14], $P_2O_7^{4-}/CO_3^{2-}$ [15], HPO_4^{2-}/SiO_3^{2-} [16].

The mineral component of bone tissue is mainly represented by carbonate-substituted hydroxyapatite [17]. Calcium hydroxyapatite $Ca_{10}(PO_4)_6(OH)_2$ is a well-known and unique ion exchanger [18–20], therefore, various cations such as Na^+, K^+, Mg^{2+}, Zn^{2+}, Ba^{2+}, or Sr^{2+} [21] and anions such as CO_3^{2-} or SiO_4^{4-}, F^- or Cl^- can be included in the composition of bone tissue [22,23].

Various powders obtained by one of the methods of chemical synthesis are used for the manufacture of bone implants [24]. Precipitation from solutions including a hydrophosphate ion, a carbonate ion, and a calcium ion is preferable due to the possibility of obtaining powders similar in chemical and phase composition to natural bone tissue [12–14,25]. Powders of calcium phosphates with molar ratio Ca/P<1.67 and calcium carbonates are used to creating materials for temporary bone implants. At the same time, hydroxyapatite-based materials (molar ratio Ca/P=1.67) are resistant to dissolution and can be used as implants for long time substituting [26].

Materials based on calcium carbonates [27–29] and calcium phosphates with a molar ratio of Ca/P<1.67 are able to dissolve gradually during implantation and therefore they are used in regenerative methods of bone defects treating [30]. Synthetic powders of calcium carbonate $CaCO_3$ and calcium phosphates with a molar ratio of Ca/P<1.67 can be used as fillers in biocompatible and biodegradable composites with polymer [31] or mineral (obtained as a result of chemical bonding reactions) matrices [32]. In addition, these powders can also be used to produce biocompatible ceramic materials with the phase composition belonging to oxide systems, including calcium oxide and phosphorus oxide [33].

The aim of the present work consisted in preparing and investigating powders synthesized from an aqueous solution of calcium chloride $CaCl_2$ and a mixed anionic solution containing orthophosphate and carbonate ions. Potassium hydroorthophosphate K_2HPO_4 was used as the source of orthophosphate ions, and potassium carbonate K_2CO_3 was used as the source of carbonate ions. For comparison, as references, powders were also synthesized from an aqueous solution of calcium chloride $CaCl_2$ and aqueous solutions including either potassium hydrophosphate K_2HPO_4 or potassium carbonate K_2CO_3.

2. Materials and Methods

For the synthesis of powders, calcium chloride $CaCl_2$ (CAS No. 10043-52-4, Rushim, Moscow, Russia), potassium hydrophosphate trihydrate K_2HPO_4 $3H_2O$ (CAS No. 16788-57-1, Rushim, Moscow, Russia) and potassium carbonate K_2CO_3 (CAS No. 584-08-7, Rushim, Moscow, Russia) were used.

 doi:10.20944/preprints202508.2229.v1

The following reactions were used to calculate the amounts of starting salts and expected products:

$$CaCl_2 + K_2HPO_4 \cdot 3H_2O \rightarrow CaHPO_4 \cdot 2H_2O + 2KCl + H_2O \quad (1)$$

$$CaCl_2 + 0{,}5K_2HPO_4 \cdot 3H_2O + 0{,}5K_2CO_3 \rightarrow 0{,}5CaCO_3 + 0{,}5CaHPO_4 \cdot 2H_2O + 2KCl + 0{,}5H_2O \quad (2)$$

$$CaCl_2 + K_2CO_3 \rightarrow CaCO_3 + 2KCl \quad (3)$$

The labeling and synthesis conditions of the powders from $CaCl_2$ and K_2HPO_4 and/or K_2CO_3 are shown in Table 1.

Table 1. The labeling and synthesis conditions of the powders.

Labeling of powders	**PO4**	**PO4_CO3**	**CO3**
The molar ratio of Ca/(HPO_4^{2-}+CO_3^{2-})	1	1	1
$CaCl_2$, mol	0,25	0,25	0,25
V of solution $CaCl_2$, l	0,5	0,5	0,5
C ($CaCl_2$), mol/l	0,5	0,5	0,5
$K_2HPO_4 \cdot 3H_2O$, mol	0,25	0,125	-
K_2CO_3, моль	-	0,125	0,25
V of solution, containing anions (HPO_4^{2-}) and/or (CO_3^{2-}), l	0,5	0,5	0,5
C($K_2HPO_4 \cdot 3H_2O$), mol/l	0,5	0,25	-
C(K_2CO_3), mol/l	-	0,25	0,5

500 ml of 0.5M aqueous solution of potassium hydrophosphate K_2HPO_4 (**PO4** powder); 500 ml of 0.5M aqueous solution of potassium carbonate K_2CO_3 (**CO3** powder); 500 ml aqueous solution containing 0.125M potassium hydrophosphate K_2HPO_4 and 0.125M potassium carbonate K_2CO_3 (**PO4_CO3** powder) were added to the 500 ml of 0.5M aqueous $CaCl_2$ solutions. The resulting suspensions were kept on a stirrer for 30 minutes. The resulting precipitates were separated from the mother liquor using vacuum filtration. The synthesized powders were dried in a thin layer at room temperature for a week. After drying, the powders were crushed using an agate mortar and pestle, and then passed through a polyester sieve with a mesh size of 200 microns. For the isolation of salts dissolved in the mother liquors they were dried at 40 °C for a month. The synthesized powders and isolated reaction by-products were weighed to determine their mass and to estimate the yield of synthesized powders and reaction by-products relatively to the theoretically possible amounts. Table 2 shows the quantities of the initial, expected target products and reaction by-product calculated in accordance with reactions (1-3).

Table 2. Quantities of initial, as well as expected target products and reaction by-product.

Starting reagents	**Labeling of synthesized powders**		
	PO4	**PO4_CO3**	**CO3**
$CaCl_2$, mol	0,25	0,25	0,25
$K_2HPO_4 \cdot 3H_2O$, mol	0,25	0,125	-
K_2CO_3, mol	-	0,125	0,25
Target products			
$CaHPO_4 \cdot 2H_2O$, mol	0,25	0,125	-
Mass of $CaHPO_4 \cdot 2H_2O$, g	**43,0**	**21,5**	-
$CaCO_3$, mol	-	0,125	0,25
Mass of $CaCO_3$, g	-	**12,5**	**25,0**
By-product	**Labeling of by-products**		
	PO4_by	**PO4_CO3_by**	**CO3_by**

 doi:10.20944/preprints202508.2229.v1

KCl, моль	0,5	0,5	0,5
Масса KCl, г	**37,3**	**37,3**	**37,3**
Total mass of expected products*	**80,3**	**73,1**	**62,3**

* The total mass of the expected products is defined as the sum of the mass of target products ($CaHPO_4 \cdot 2H_2O$ and/or $CaCO_3$) and mass of reaction by-product (KCl).

To study the thermal evolution of the phase composition of the synthesized powders, they were placed in porcelain boats and heated at a heating rate of 5 °C/min, followed by exposure for 2 hours at various temperatures in the range of 200-1000 °C. The labeling of the powders after heat treatment used in the figures is shown in Table 3.

Table 3. Labeling of powders obtained after heat treatment.

Temperature of heat treatment	Labeling of synthesized powders		
	PO4	**PO4_CO3**	**CO3**
200 °C	PO4_200	PO4_CO3_200	CO3_200
400 °C	PO4_400	PO4_CO3_400	CO3_400
600 °C	PO4_600	PO4_CO3_600	CO3_600
800 °C	PO4_800	PO4_CO3_800	CO3_800
1000 °C	PO4_1000	PO4_CO3_1000	-

The phase composition of powders after synthesis and after heat treatment was performed by X-ray powder diffraction (XRD) analysis using CuKa radiation (λ = 1.5418 Å, step 2θ – 0.02°) using Rigaku D/Max-2500 diffractometers (Rigaku Corporation, Tokyo, Japan) in the angle range 2θ = 2...70° or Tongda TD-3700 (Dandong Tongda Science & Technology Co., Ltd., Dandong, China) in the angle range 2θ = 3...70°. The X-ray images were analyzed using the WinXPOW program using the ICDD PDF-2 (http://www.icdd.com/products/pdf2.htm, accessed on 18 August 2025) [34] databases and the Match! program. (https://www.crystalimpact.com/, accessed on 18 August 2025). The quantitative ratio of the target and related products in the obtained powders was determined using the Match!3 program, https://www.crystalimpact.com/. The infrared (IR) spectra were collected in the wavelength range 500-4000 cm^{-1} using the Spectrum Three IR spectrometer (Perkin Elmer, Waltham, Massachusetts, USA) in the mode of disturbed total internal reflection using the Universal ATR accessory (crystal diamond/KRS-5). The bands in the spectra were assigned based on the literature data [35]. Synchronous thermal analysis (TA), including thermogravimetric analysis (TGA) and differential scanning calorimetry (DSC), was performed on a NETZSCH STA 449 F3 Jupiter thermal analyzer (NETZSCH, Selb, Germany) in air in the temperature range of 40-1000 °C at a heating rate of 10 °C/min, using pre-thermostating at 40 °C for 30 minutes. The mass of the sample was at least 10 mg. The composition of the gas phase was monitored using a Netzsch QMS 403 Quadro quadrupole mass spectrometer (NETZSCH, Germany) combined with a NETZSCH STA 449 F3 Jupiter thermal analyzer (NETZSCH, Selb, Germany). Mass spectra (MS) were recorded for m/z=44 (CO_2). The microstructure of the powders was studied by scanning electron microscopy (SEM) using a scanning electron microscope with an auto emission source JEOL JSM-6000PLUS Neoscope II (JEOL Ltd., Japan). For the study, the samples were glued onto a copper substrate using carbon tape, and a layer of gold ~ 15nm was sprayed. The survey was carried out in vacuum mode. The accelerating voltage of the electron gun was up to 5 kV. The images were obtained in secondary electrons at magnifications up to 1000× and recorded in digitized form on a computer.

3. Results and Discussion

The XRD data of synthesized powders are shown in Figure 1.

 doi:10.20944/preprints202508.2229.v1

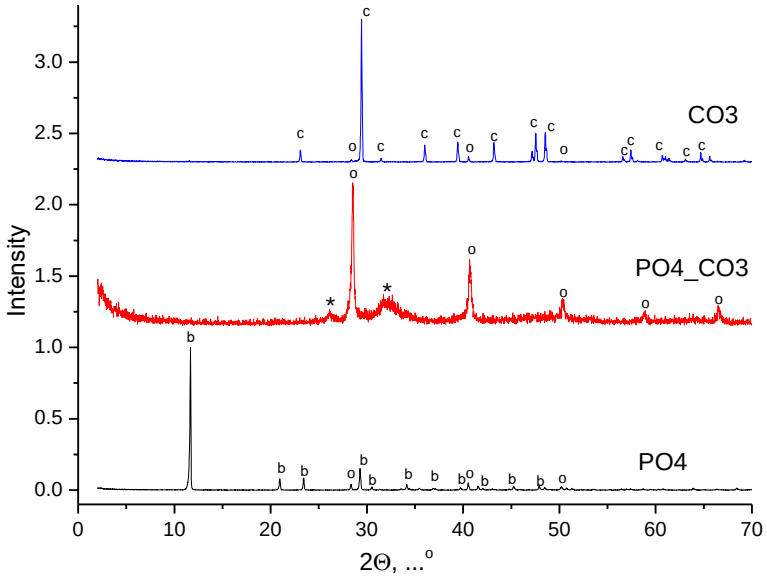

Figure 1. XRD data of synthesized powders: c – calcium carbonate (calcite) $CaCO_3$ (PDF card No 5-586; No 96-210-0190); o – potassium chloride (sylvine) KCl (PDF card No 41-1476; No 96-900-8652); * - hydroxyapatite $Ca_{10}(PO_4)_6(OH)_2$ (PDF card No 9-432, No 96-900-1234); b – brushite $CaHPO_4{\cdot}2H_2O$ (PDF card No 9-77; No 96-231-0527).

Phase composition of powder, synthesized from water solutions $CaCl_2$ and K_2CO_3, included calcite $CaCO_3$. Phase composition of powder, synthesized from water solutions $CaCl_2$ and K_2HPO_4, included brushite $CaHPO_4{\cdot}2H_2O$. Phase composition of powder, synthesized from water solutions $CaCl_2$ and mixed-anionic solution containing K_2CO_3 и K_2HPO_4, included a low crystalline product with the main peaks corresponding to hydroxyapatite $Ca_{10}(PO_4)_6(OH)_2$. All synthesized powders included potassium chloride (sylvine) KCl as a reaction by-product. XRD data of reaction by-products isolated from mother liquors is presented in Figure 2. The phase composition of the by-products isolated from the mother liquors was presented by potassium chloride (sylvine) KCl.

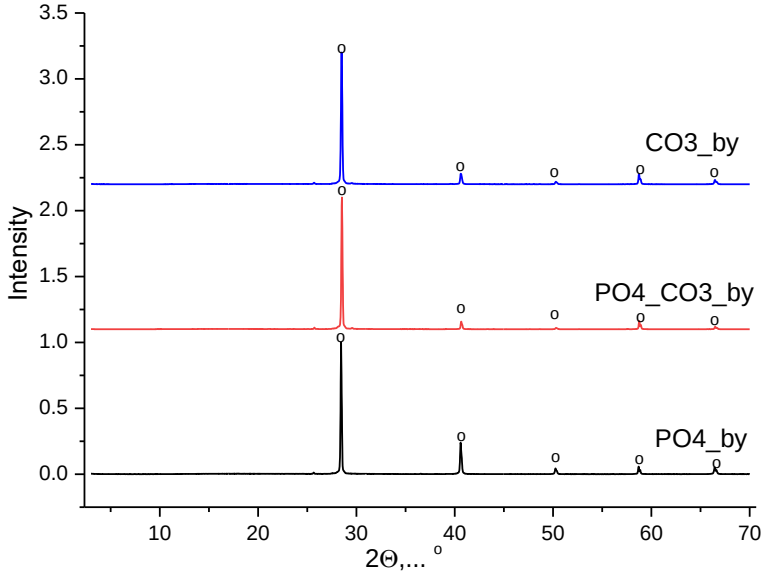

Figure 2. XRD data of products isolated from mother liquors after synthesis: o – potassium chloride (sylvine) KCl (PDF card No 41-1476; No 96-900-8652).

 doi:10.20944/preprints202508.2229.v1

The formation of brushite $CaHPO_4 \cdot 2H_2O$ and calcite $CaCO_3$ can be caused by reactions (1) and (3), respectively. During the preparation of the mixed-anionic aqua solution from potassium hydrophosphate K_2HPO_4 and potassium carbonate K_2CO_3 taken in an equimolar ratio, not only the release of CO_2 was observed, but also the formation of potassium orthophosphate K_3PO_4, occurred. Reaction (4) indicates that when mixing solutions of these two salts the presence of potassium carbonate K_2CO_3 also persists.

$$2K_2HPO_4 + K_2CO_3 \rightarrow 2K_3PO_4 + H_2O + CO_2 \quad (4)$$

So, due to hydrolysis (reactions 5 and 6) the mixed-anionic solution had an alkaline pH, characteristic of aqua solution of salts formed by a strong base and a weak acid:

$$K_2CO_3 + 2H_2O \rightarrow KHCO_3 + KOH + H_2O \quad (5)$$

$$K_3PO_4 + H_2O \rightarrow K_2HPO_4 + KOH \quad (6)$$

The synthesis of hydroxyapatite can be represented formally as reaction (7) taking into account the molar ratio of the salts used for synthesis as it was described in Materials and methods (reaction 2):

$$12CaCl_2 + 6K_2HPO_4 + 6K_2CO_3 \rightarrow Ca_{10}(PO_4)_6(OH)_2 + 2CaCO_3 + 24KCl + 2H_2O + 4CO_2 \quad (7)$$

In this case, the theoretically possible amount of hydroxyapatite $Ca_{10}(PO_4)_6(OH)_2$ (0.0208 mol=20.9 g) can be calculated as 1/6 of the amount of potassium hydrophosphate K_2HPO_4 (0.125 mol) used for preparation of a mixed-anionic solution (Table 1). Taking into account the possibility of formation of calcium carbonate $CaCO_3$, the mass of the precipitate can be calculated as the sum of the possible amounts of hydroxyapatite and calcium carbonate. The amount of calcium carbonate $CaCO_3$ (0.0417 mol=4.17 g) can be calculated as 1/6 of the amount of $CaCl_2$ (0.25 mol). Thus, the mass of the precipitate in the synthesis of **PO4_CO3** can be calculated as 25.07 g. Theoretically calculated (expected) and experimentally obtained masses of target products and by-products, as well as their comparison, are presented in Table 4.

Table 4. The expected and obtained masses of synthesized powders and reaction by-products.

Labeling	PO4	PO4_CO3	CO3
The expected quantities of target products and by-product:			
$CaHPO_4 \cdot 2H_2O$, g	43,0	-	-
$Ca_{10}(PO_4)_6(OH)_2 + CaCO_3$, g	-	25,1	-
$CaCO_3$, g	-	-	25,0
KCl, g	37,3	37,3	37,3
Total mass of expected products *, g	**80,3**	**62,4**	**62,3**
The obtained masses of the synthesized powders and the extracted by-products:			
Mass of the powders after drying, g	43,0	33,5	17,4
Mass of the extracted reaction by-product, g	30,6	25,5	37,1
Total mass of prepared products**, g	**73,6**	**59,0**	**54,5**
The yield of synthesized products	91,7%	94,5%	87,5%
The yield of reaction by-product	82,0%	68,4%	99,4%
Mass of by-product, preserved by precipitate (estimation), g	**6,7**	**11,8**	**0,2**
Content of by-product in powders (estimation)	**15,6%**	**35,2%**	**1,1%**
Content of by-product in powders (estimation according to Match!)	**2.8%**	**30.9%**	**1,8%**

* Total mass of expected products was determent as sum of target product ($CaHPO_4 \cdot 2H_2O$ and/or $CaCO_3$) and reaction by-product (KCl). ** Total mass of prepared products was determined as sum of mass powder after drying and mass of the product extracted from mother liquor.

 doi:10.20944/preprints202508.2229.v1

The data presented in the Table 4 indicate that the total yield of synthesis products was close to ~90% in all cases. According to the estimation obtained using the Match! program, the content of the reaction by-product (potassium chloride, sylvine KCl) was maximal (30.9%) in the powder synthesized from a mixed-anionic solution. The amount of potassium chloride (sylvine) KCl in the **PO4** powder was determined as 2.8%, and in the **CO3** powder it was determined as 1.8%. The estimation of the amount of by-product in synthesized powders obtained using the Match! program is consistent with the estimation of the amount of by-product retained in **PO4_CO3** and **CO3** powders (Table 4). A small particle size and a significant specific surface area may determine the ability of the synthesized **PO4_CO3** powder to retain (occlude) mother liquors and the by-product dissolved in it, as it has been shown in other studies [36].

Figure 3 shows the FTIR spectroscopy data of synthesized powders.

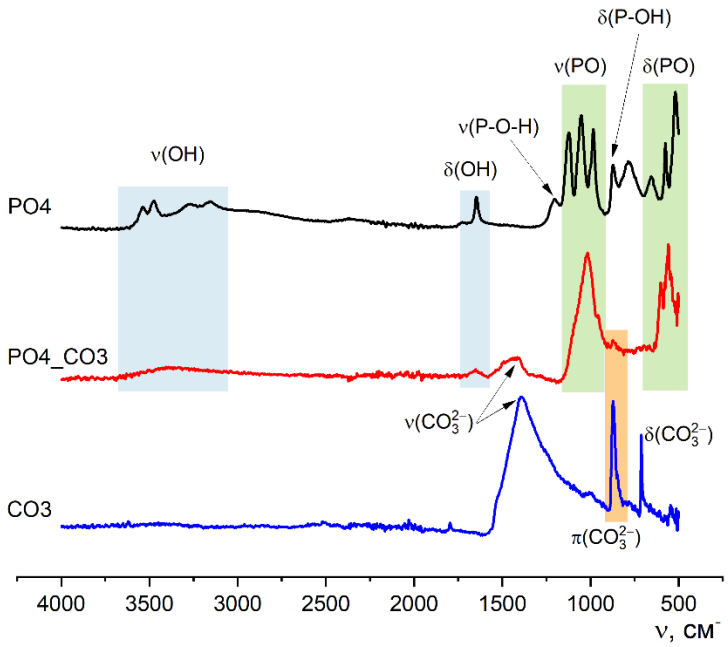

Figure 3. FTIR spectra of synthesized powders **PO4**, **PO4_CO3**, **CO3**.

The FTIR spectroscopy data (Figure 3) is consistent with the X-ray diffraction data, since the appearance of the curves corresponds to the reference and literature data for brushite (SpectraBase Spectrum ID 9u0yn3G2J6i https://spectrabase.com/spectrum/9u0yn3G2J6i [37–39]), calcite (SpectraBase Compound ID YYVCfbcpX1 https://spectrabase.com/spectrum/YYVCfbcpX1 [40–42]), hydroxyapatite (SpectraBase Spectrum ID BxeLPnr9PTc https://spectrabase.com/spectrum/BxeLPnr9PTc [43], and carbonate-hydroxyapatite [14,44,45]). On the spectra of **PO4** and **CO3** powders, there are valence (ν) and deformation (δ) vibrations which are characteristic of brushite $CaHPO_4{\cdot}2H_2O$: ν(OH) – 3539, 3473, 3270, 3153 $см^{-1}$; ν(P-O-H) – 1204 $см^{-1}$; ν(PO) – 1120, 1052, 980 $см^{-1}$ δ(OH) – 1645 $см^{-1}$; 980 $см^{-1}$; δ(P-OH) – 871 $см^{-1}$; δ(PO) – 656, 575, 519 $см^{-1}$) and calcite $CaCO_3$: $\nu(CO_3^{2-})$ – 1390 $см^{-1}$; $\pi(CO_3^{2-})$ – 874 $см^{-1}$; $\delta(CO_3^{2-})$ – 710 $см^{-1}$) respectively.

Characteristic vibrations of the phosphate group PO_4^{3-}, which confirm the formation of weakly crystallized hydroxyapatite, can also be seen on the spectrum of the powder **PO4_CO3**. Vibrations of $\nu(CO_3^{2-})$ – 1410 $см^{-1}$; and $\pi(CO_3^{2-})$ – 874 $см^{-1}$ in the spectrum of **PO4_CO3** powder suggest the presence of carbonate groups in the structure of the synthesized low crystalline hydroxyapatite. The presence of potassium chloride KCl, regardless of its content in the synthesized powders, is not determined due to the absence of absorption bands in the studied region [46,47].

Figure 4 shows micrographs of synthesized powders.

 doi:10.20944/preprints202508.2229.v1

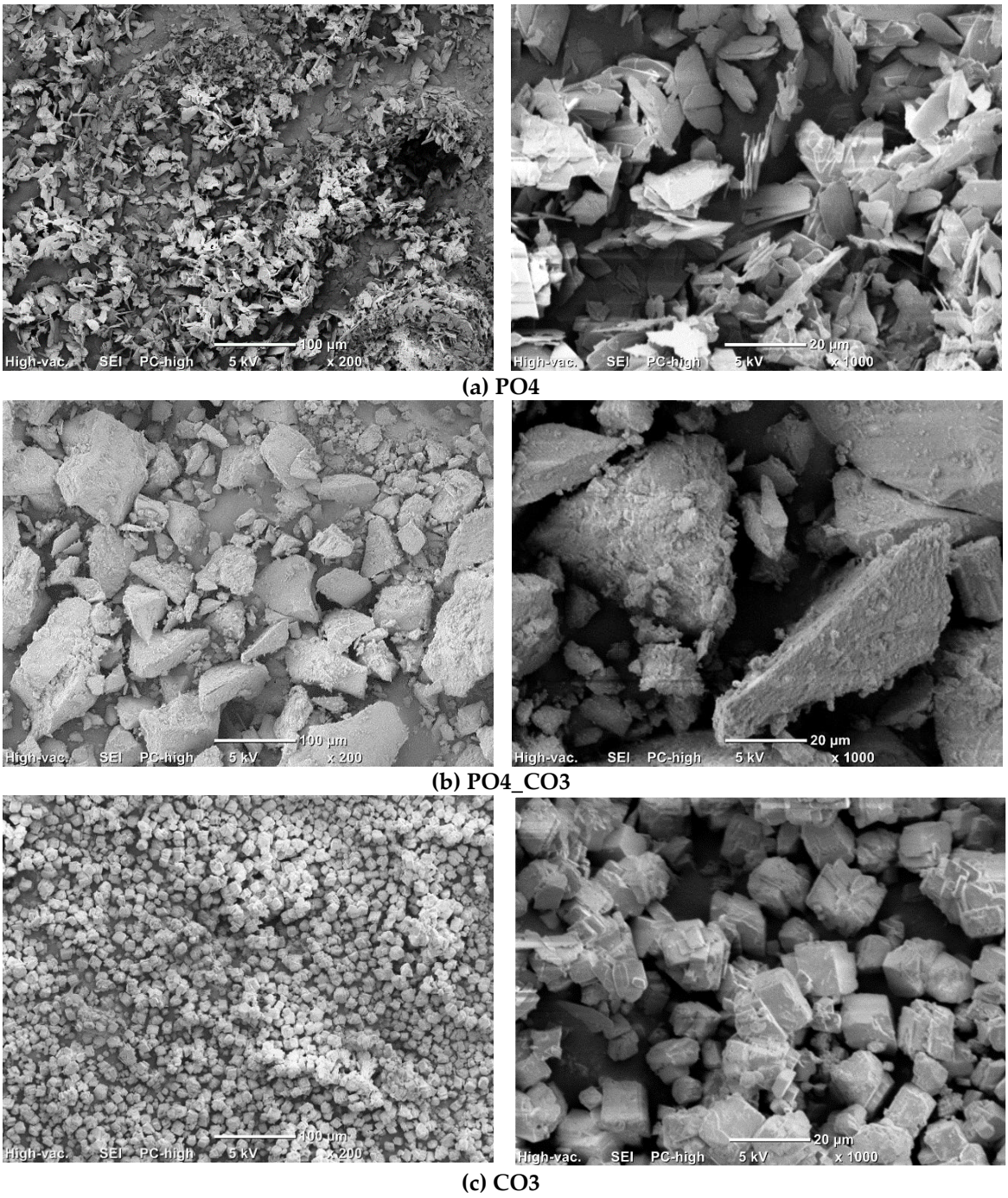

Figure 4. Micrographs of synthesized powders **PO4** (a), **PO4_CO3** (b), **CO3** (c).

The particles of **PO4** powder (Figure 4, a) with a size of 10-20 microns and a thickness of 1-2 µm have a lamellar morphology characteristic for brushite $CaHPO_4 \cdot 2H_2O$ [48]. The particles of **CO3** powder (Figure 4, c) with a size of 10-20 µm have the cubic shapes which is one of typical for calcite $CaCO_3$ [49]. The powder **PO4_CO3** (Figure 4, b) is composed of large aggregates of 5-60 µm in size, consisting of particles less than 1 µm in size. Hydroxyapatite powders synthesized by precipitation from solutions, as a rule, consist of particles having a size of less than a micron [44]. It was estimated that the mass (33.5 g) of the synthesized **PO4_CO3** powder after drying was 8.4 g higher than the expected (25.1 g) mass of the powder (Table 4). The mass of reaction by-product (**PO4_CO3_by**) isolated from the mother liquor was 11.8 g less than the expected (37.3 g) mass. Thus, after drying and grinding in a mortar, KCl (reaction by-product) retaining in synthesized powder acted as a binder, binding hydroxyapatite particles in large aggregates visible in the micrographs (Figure 4, b).

 doi:10.20944/preprints202508.2229.v1

Figure 5 shows the TA data of the synthesized powders. According to the TGA data (Figure 5, a), the total weight loss at 1000 °C for **PO4** powder was 27.9%. The change in the weight of the PO4 powder is possible due to the removal of physically bounded water, dehydration of brushite $CaHPO_4 \cdot 2H_2O$ and the formation of monetite $CaHPO_4$ (reaction 8), and the conversion of monetite $CaHPO_4$ into $Ca_2P_2O_7$ pyrophosphate (reaction 9).

$$CaHPO_4 \cdot 2H_2O \rightarrow CaHPO_4 + 2H_2O \quad (8)$$

$$2CaHPO_4 \rightarrow Ca_2P_2O_7 + H_2O \quad (9)$$

The theoretically possible mass loss during reactions 8 and 9 is 26.16%, which is close to the value of the total mass loss for **PO4** powder determined by the TGA method. All the processes indicated for the **PO4** powder, leading to weight loss, occur with heat absorption in the ranges 87-168 °C, 168-243 °C, 375-477 °C (Figure 5, b). It can be assumed that the presence of KCl in the **PO4** powder, as well as the stage of thermostating the sample at 40 °C for 30 minutes before heating at a set rate (10 °C/min), causes decomposition of the metastable brushite at lower temperatures in the range of 87-168 °C (reaction 8). In article [50] the authors conclude that two-stage conversion of brushite into monetite was possible with formation of an amorphous phase at the first stage. The range 168-243 °C should be considered as characteristic of the monetite $CaHPO_4$ formation from brushite $CaHPO_4 \cdot 2H_2O$; and the range 375-477 °C should be considered as characteristic of the calcium pyrophosphate $Ca_2P_2O_7$ from $CaHPO_4$ monetite formation [51]. In the range of 477-840 °C, the smooth change in mass was 3%, while it is difficult to identify the intervals for processes occur with heat absorption or release.

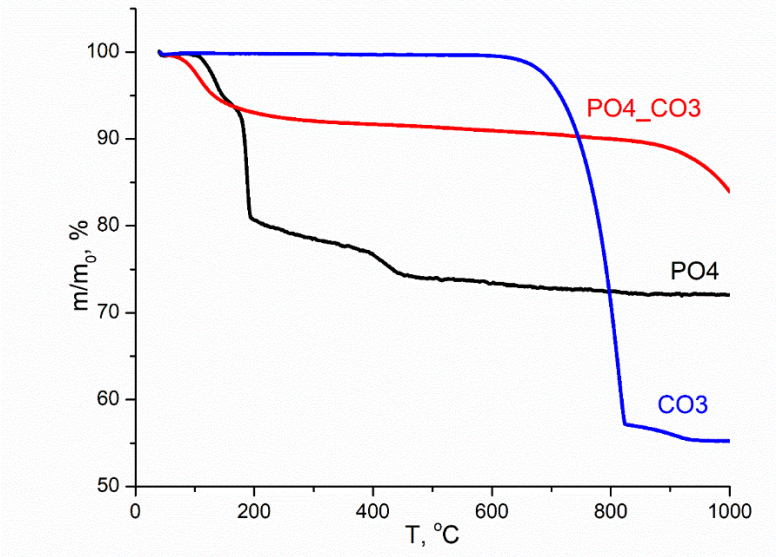

(a)

 doi:10.20944/preprints202508.2229.v1

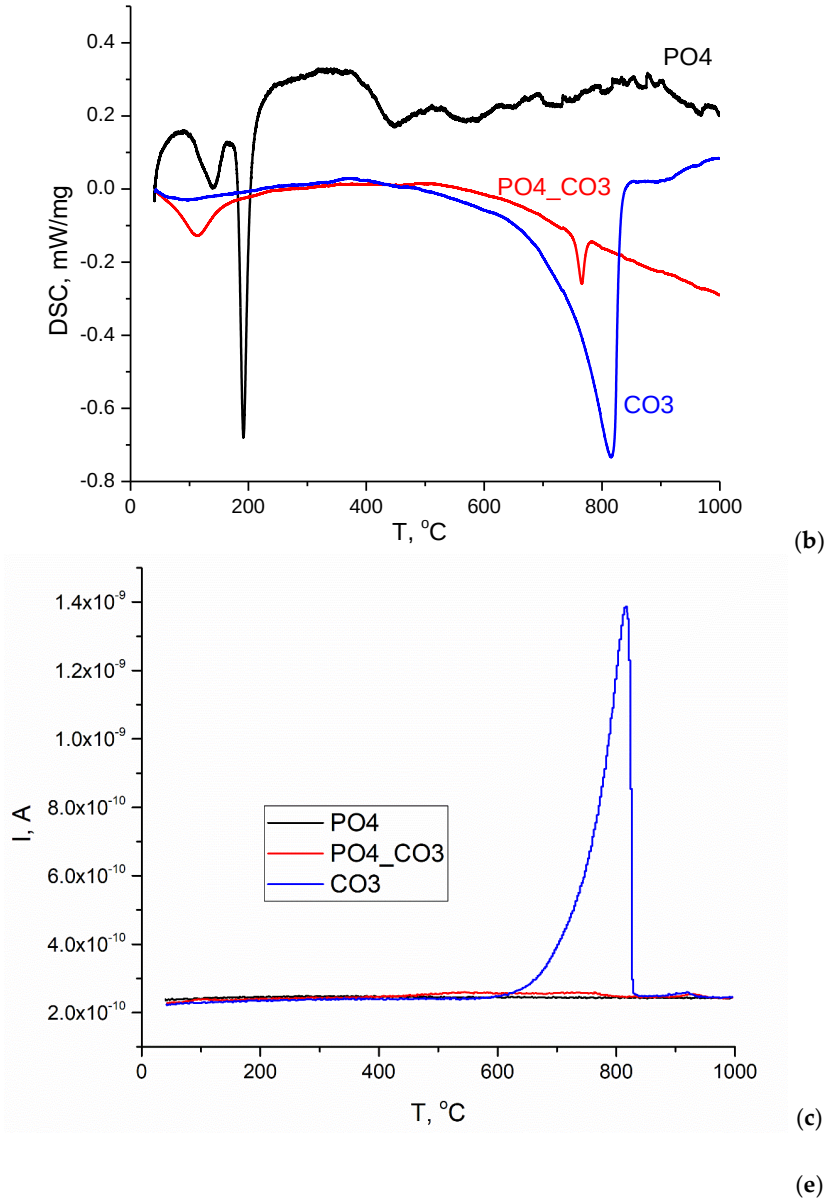

Figure 5. TA data of synthesized powders: TGA (a), DSC (б), MS for m/z=44 (CO_2).

According to the TGA data (Figure 5, a), the total weight loss at 1000 °C for the **CO3** powder was 44.9%. The theoretically possible mass change for calcite during thermal decomposition in accordance with reaction (10) is 44%. The change in the mass of the **CO3** powder occurred with heat absorption in the range 622-844 °C, amounted to 42.9% due to the decomposition of calcite and was accompanied by the release of CO_2 (reaction 10).

$$CaCO_3 \rightarrow CaO + CO_2 \quad (10)$$

The graph of the mass change of the **CO3** powder (Figure 5, a) and the dependence of the ion current on temperature (Figure 5, c) have the forms characteristic for calcite $CaCO_3$ [52]. In Figure 5, c, for the **CO3** powder, one can see a graph of the dependence of the ion current on temperature for m/z=44 (CO_2), typical for $CaCO_3$. It should be noted that in the range 844-949 °C, a loss (2%) of mass is observed, which is most likely associated with both the removal of CO_2 and the removal of that insignificant amount of KCl (Table 4), which could be captured by the synthesized **CO3** powder above the melting point of KCl (776 °C [53] or 769 ± 2 °C (1042 ± 2 K) [54]).

According to the TGA data (Figure 5, a), the total weight loss at 1000 °C for **PO4_CO3** powder was 16.2%. Three sections can be distinguished on the curve of mass versus temperature for

 doi:10.20944/preprints202508.2229.v1

PO4_CO3 powder: removal of physically bound water (7.5% mass loss), which proceeds with heat absorption in the range of 43-240 °C; a section of smooth weight reduction (2.6%) in the range of 240-829 °C; and a section of mass loss (6.1%), apparently related to the removal of KCl, in the range of 829-1000 °C. The endothermic peak at 765 °C clearly seen on the DSC curve (Figure 5, b) can be attributed to the melting of KCl, since according to the estimate (Table 4), the mass of the retained reaction by-product (KCl) in the **PO4_CO3** powder was the maximum. No endothermic peaks that could be attributed to the KCl melting process were found in the DSC graphs for **PO4** and **CO3** powders synthesized for comparison. Significantly lower values of the ion current can be seen on the curve m/z =44 (CO2) for **PO4-CO3** powder (Figure 5, c) in wide ranges of 460-800 °C and 900-940 °C than for **CO3** powder.

Figure 6 shows the XRD of the **CO3** powder synthesized from aqueous solutions of $CaCl_2$ and K_2CO_3 after heat treatment at various temperatures.

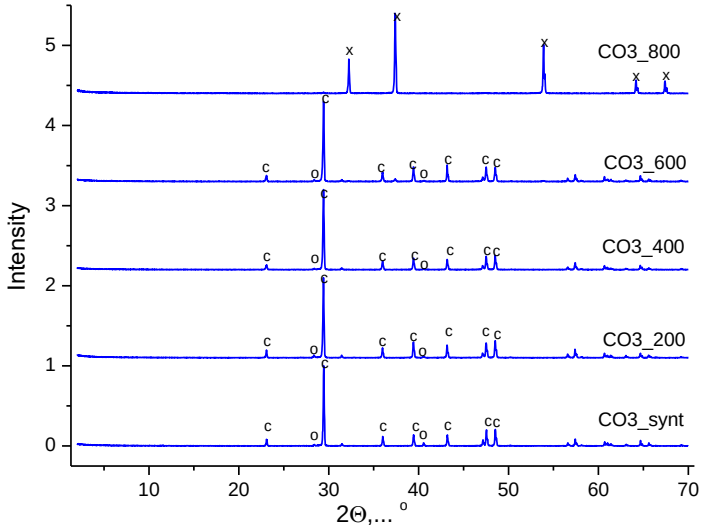

Figure 6. XRD data of **CO3** powder after synthesis and after heat treatment at different temperatures. c – calcium carbonate (calcite) $CaCO_3$ (PDF card No 5-586; No 96-210-0190); o - potassium chloride (sylvine) KCl (PDF No 41-1476; No 96-900-8652); x – calcium oxide CaO (PDF No 37-1497, No 96-101-1096).

According to the XRD data, the phase composition of the **CO3** powder synthesized from aqueous solutions of $CaCl_2$ and K_2CO_3, after heat treatment at various temperatures in the range of 200-600 °C for 2 hours, was represented by calcite $CaCO_3$. And after heat treatment at 800 °C, the phase composition of the **CO3** powder was represented by calcium oxide CaO (reaction 10).

Figure 7 shows micrographs of **CO3** powders after heat treatment for 2 hours at various temperatures in the range of 200-600 °C. The particle size and shape of the powder particles after heat treatment does not significantly differ from the particle size and shape of the synthesized powder. It is difficult to detect particles with dimensions less than 2 μm and more than 20 μm in the micrographs.

 doi:10.20944/preprints202508.2229.v1

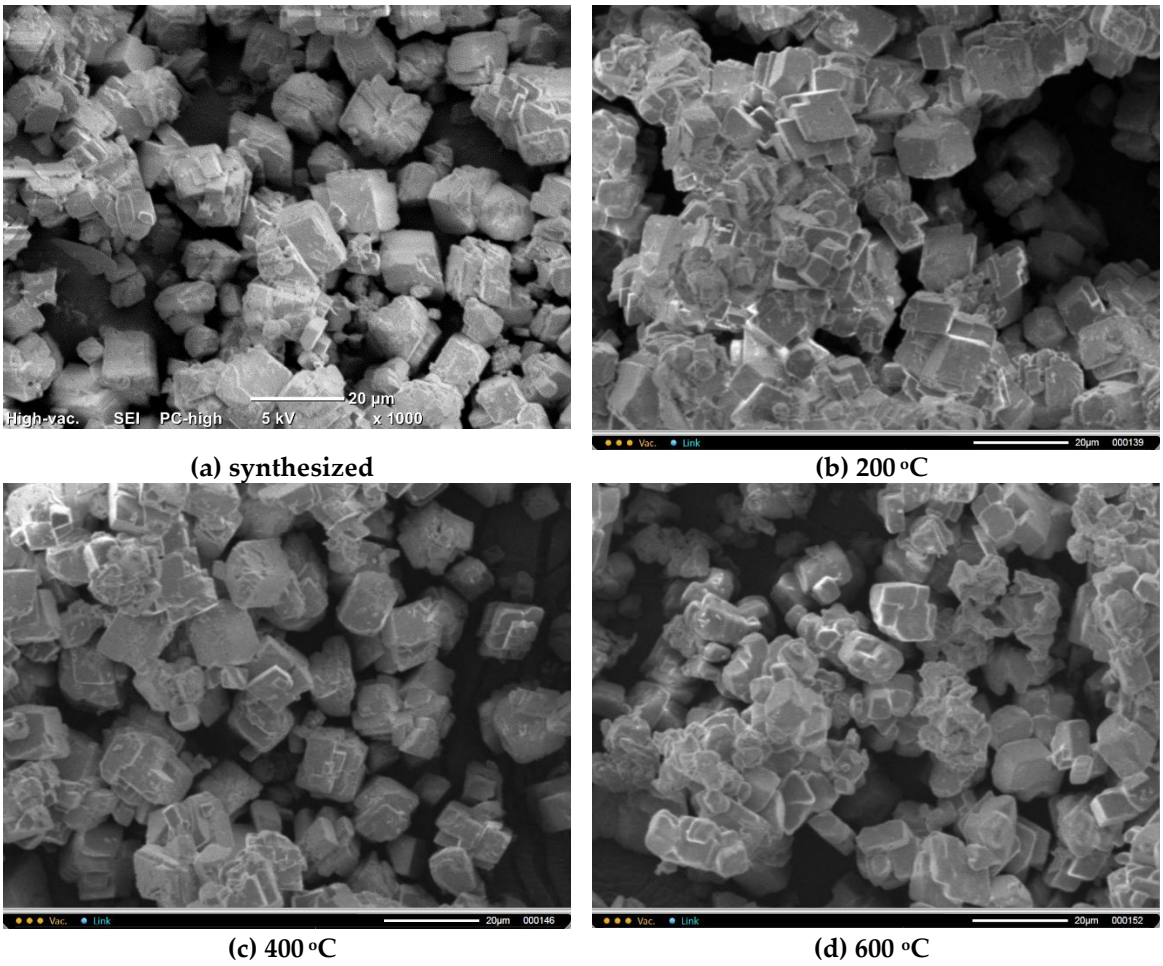

Figure 7. Microphotographs of **CO3** powder after synthesis (a) and after heat treatment at different temperatures 200 °C (b), 400 °C (c), 600 °C (d).

Figure 8 shows the XRD of **PO4** powder synthesized from aqueous solutions of $CaCl_2$ and K_2HPO_4 after heat treatment at various temperatures. After heat treatment at 200 °C for 2 hours, the phase composition of the **PO4_200** powder is represented by monetite $CaHPO_4$ (reaction 9). The phase composition of the **PO4_400** and **PO4_600** powders was represented by γ-calcium pyrophosphate γ-$Ca_2P_2O_7$ (reaction 10) after heat treatment at 400 °C and at 600 °C for 2 hours. The phase composition of the **PO4_800** and **PO4_1000** powders included β-tricalcium phosphate β-$Ca_3(PO_4)_2$, β-calcium pyrophosphate β-$Ca_2P_2O_7$, as well as calcium potassium pyrophosphate $K_2CaP_2O_7$ after heat treatment at 800 °C and at 1000 °C for 2 hours

 doi:10.20944/preprints202508.2229.v1

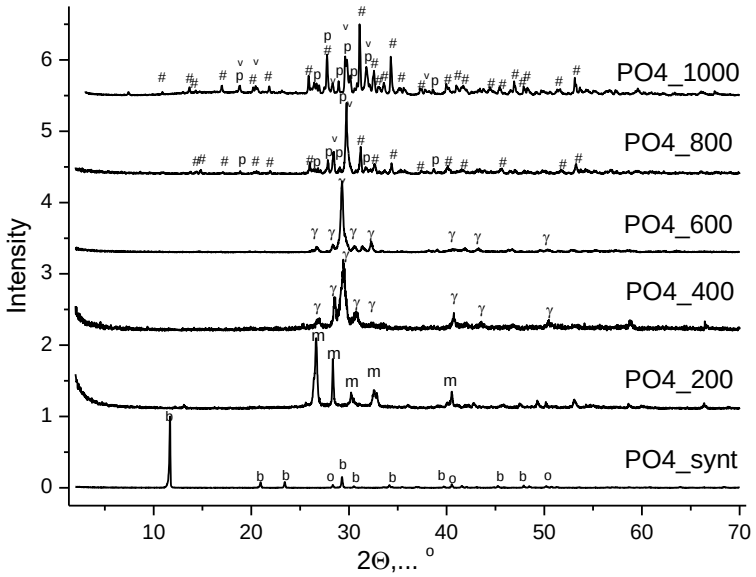

Figure 8. XRD data of powder **PO4** b after synthesis and after heat treatment at different temperatures. o - potassium chloride (sylvine) KCl (PDF No 41-1476; No 96-900-8652); b – brushite $CaHPO_4 \cdot 2H_2O$ (PDF card No 9-77; No 96-231-0527); m – monetite $CaHPO_4$ (PDF card No 9-80; 96-210-6185); γ - γ-calcium pyrophosphate γ-$Ca_2P_2O_7$ (PDF card No 17-499); p - β- calcium pyrophosphate β-$Ca_2P_2O_7$ (PDF card 9-346; No 96-100-1557); # - β-tricalcium phosphate β-$Ca_3(PO_4)_2$ (PDF card No 9-169; No 96-151-7239) v – $K_2CaP_2O_7$ (PDF card No 22-805; No 96-220-2941).

Reaction (11) may reflect the formation of β-calcium orthophosphate β-$Ca_3(PO_4)_2$ and calcium potassium pyrophosphate $K_2CaP_2O_7$:

$$2Ca_2P_2O_7 + 2KCl + H_2O \rightarrow Ca_3(PO_4)_2 + K_2CaP_2O_7 + 2HCl \quad (11)$$

Figure 9 shows micrographs of **PO4** powders after thermal treatment for 2 hours at various temperatures in the range of 200-1000 °C. The particle size and shape of the powder particles after heat treatment at 200 and 400 ° C practically does not differ from the particle size and shape of the synthesized powder. After heat treatment in the range of 600-1000 °C, as the temperature increases, the powder particles more and more lose their lamellar morphology. And after heat treatment at 1000 °C, the **PO4_1000** powder is composed of conglomerates 5-20 microns in size, consisting of particles 1-3 microns in size, sintered together.

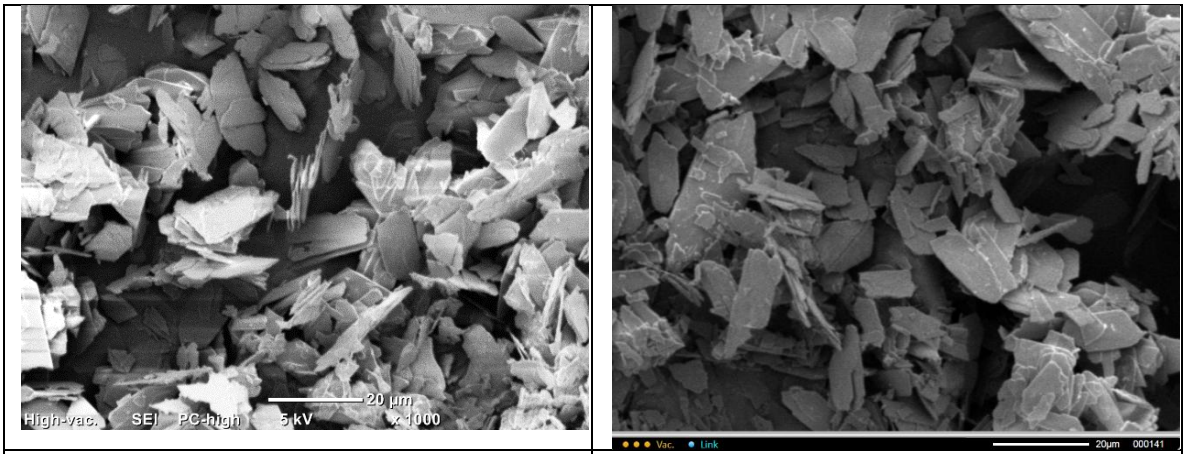

(a) synthesized PO4 | **(b) PO4_200**

 doi:10.20944/preprints202508.2229.v1

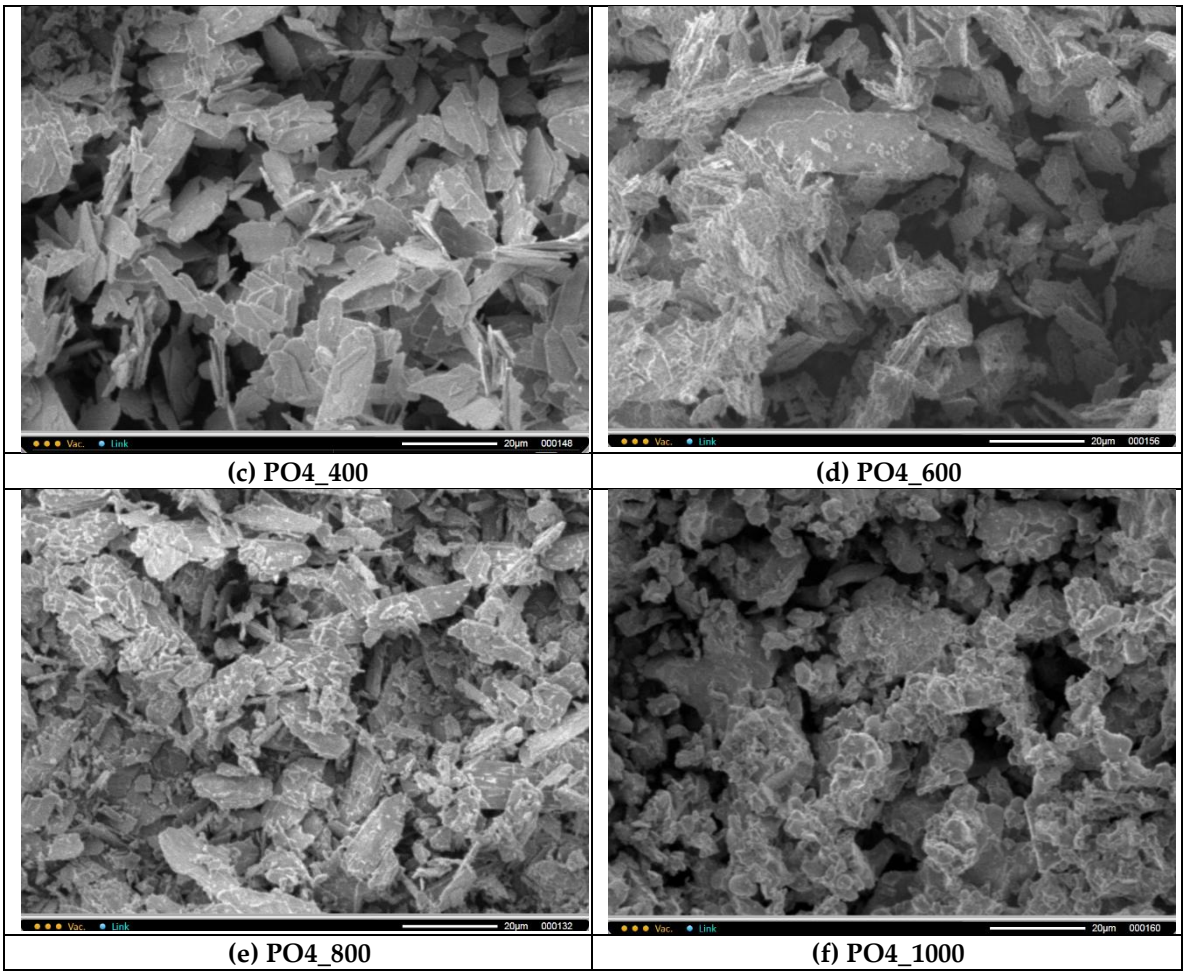

Figure 9. Micrographs of **PO4** powder after synthesis (a) and after heat treatment at various temperatures: 200 (b), 400 (c), 600 (d), 800 (e), 1000 (f).

Figure 10 shows the FTIR data for **PO4** and **PO4_1000** powders, along with the XRD and SEM data, confirming the transformation of the synthesized powder after heat treatment at 1000 °C. After heat treatment of the **PO4** powder at 1000 °C, according to the FTIR data, the presence of PO_4^{3-} groups remains and a δ(POP) 720 cm^{-1} vibration appears, which confirms the presence of the pyrophosphate ion $P_2O_7^{4-}$ in both calcium pyrophosphate formed from brushite (reactions 8 and 9) and calcium potassium pyrophosphate (reaction 11).

 doi:10.20944/preprints202508.2229.v1

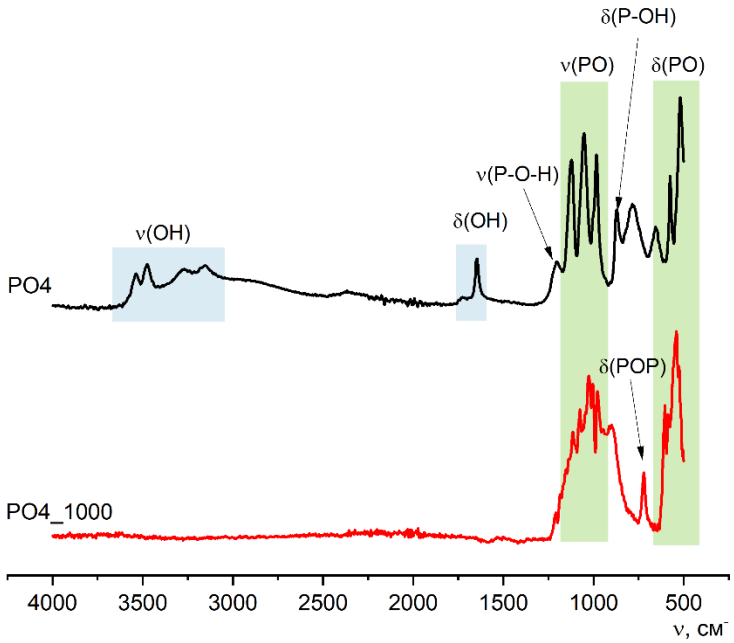

Figure 10. FTIR spectra of synthesized **PO4** powder and powder **PO4_1000** after heat treatment at 1000 °C.

Figure 11 shows the XRD of the **PO4_CO3** powder synthesized from aqueous solutions of $CaCl_2$, $KHPO_4$ and K_2CO_3 after heat treatment at various temperatures. The phase composition of **PO4_CO3** powders after thermal treatment in the range of 200-800 °C is represented by weakly crystallized hydroxyapatite and potassium chloride (sylvine) KCl. After heat treatment at 1000 °C, the phase composition of the powder **PO4_CO3_1000** is represented by chlorapatite $Ca_{10}(PO_4)_6Cl_2$. The formation of chlorapatite can be reflected by the reaction (12):

$$Ca_{10}(PO_4)_6(OH)_2 + 2KCl \rightarrow Ca_{10}(PO_4)_6Cl_2 + 2KOH \quad (12)$$

A similar formation of chlorapatite was observed at 1000 °C from weakly crystalline hydroxyapatite of natural origin and sodium chloride NaCl [55].

Micrographs of **PO4_CO3** powder after synthesis and after heat treatment at various temperatures are presented in Figure 12. The microstructure of **PO4_CO3** powders, after thermal treatment in the range of 200-800 °C, does not significantly differ from the microstructure of the powder after synthesis and drying. Powders consist of sufficiently large agglomerates (up to 100-200 μm) consisting of particles of weakly crystallized hydroxyapatite bonded with reaction by-product KCl. The microstructure of the **PO4_CO3_1000** powder after heat treatment at 1000 °C differs significantly from the microstructure of powders after heat treatment in the range of 200-800 °C. The **PO4_CO3_1000** powder after heat treatment at 1000 °C consists of particles with a prismatic shape 5-20 μm long and a transverse dimension of 2-5 μm. In the micrograph (Figure 12, e, left side) with a lower magnification, one can see loose aggregates up to 100 microns in size, consisting of mentioned above prismatic particles.

 doi:10.20944/preprints202508.2229.v1

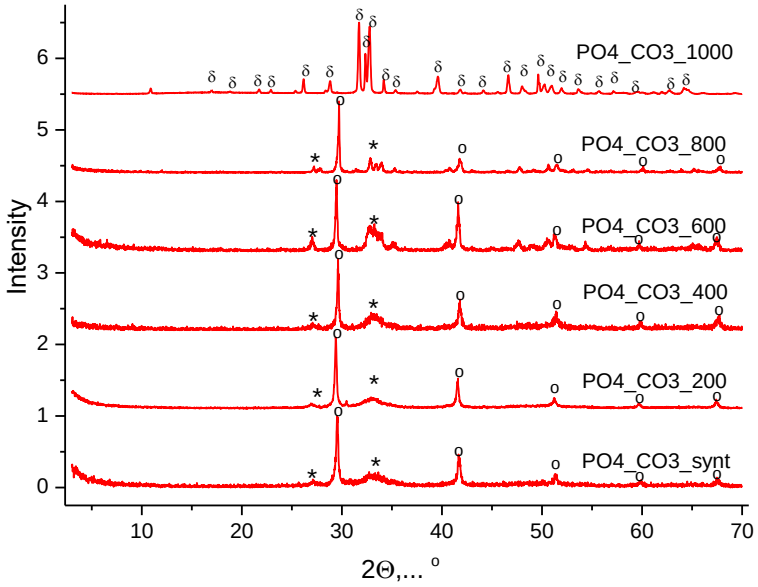

Figure 11. XRD data of **PO4_CO3** powder after synthesis and after heat treatment at different temperatures. * - hydroxyapatite $Ca_{10}(PO_4)_6(OH)_2$ (PDF No 96-901-4314) o - potassium chloride (sylvine) KCl (PDF No 41-1476; No 96-900-8652); δ – chlorapatite $Ca_{10}(PO_4)_6Cl_2$ (PDF No 73-1728; No 96-101-0917).

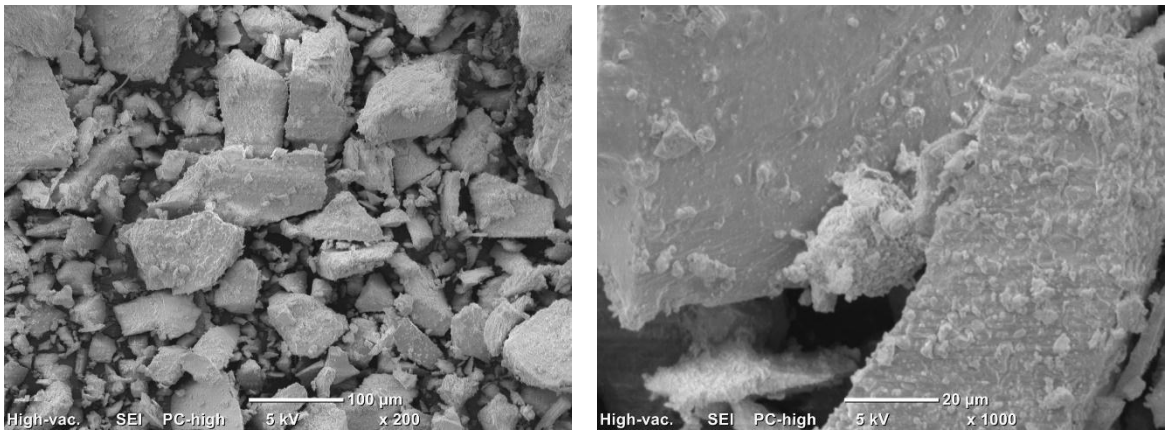

200 °C (a)

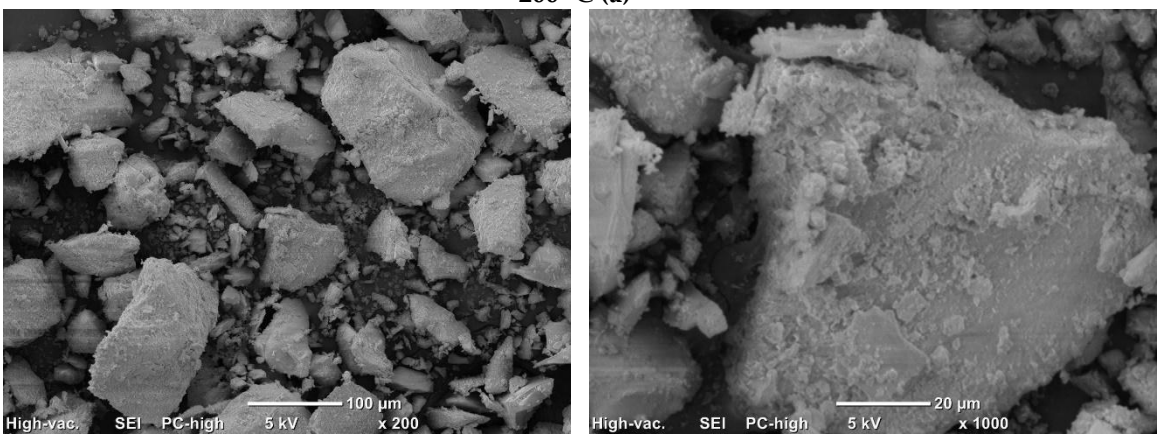

400 °C (b)

 doi:10.20944/preprints202508.2229.v1

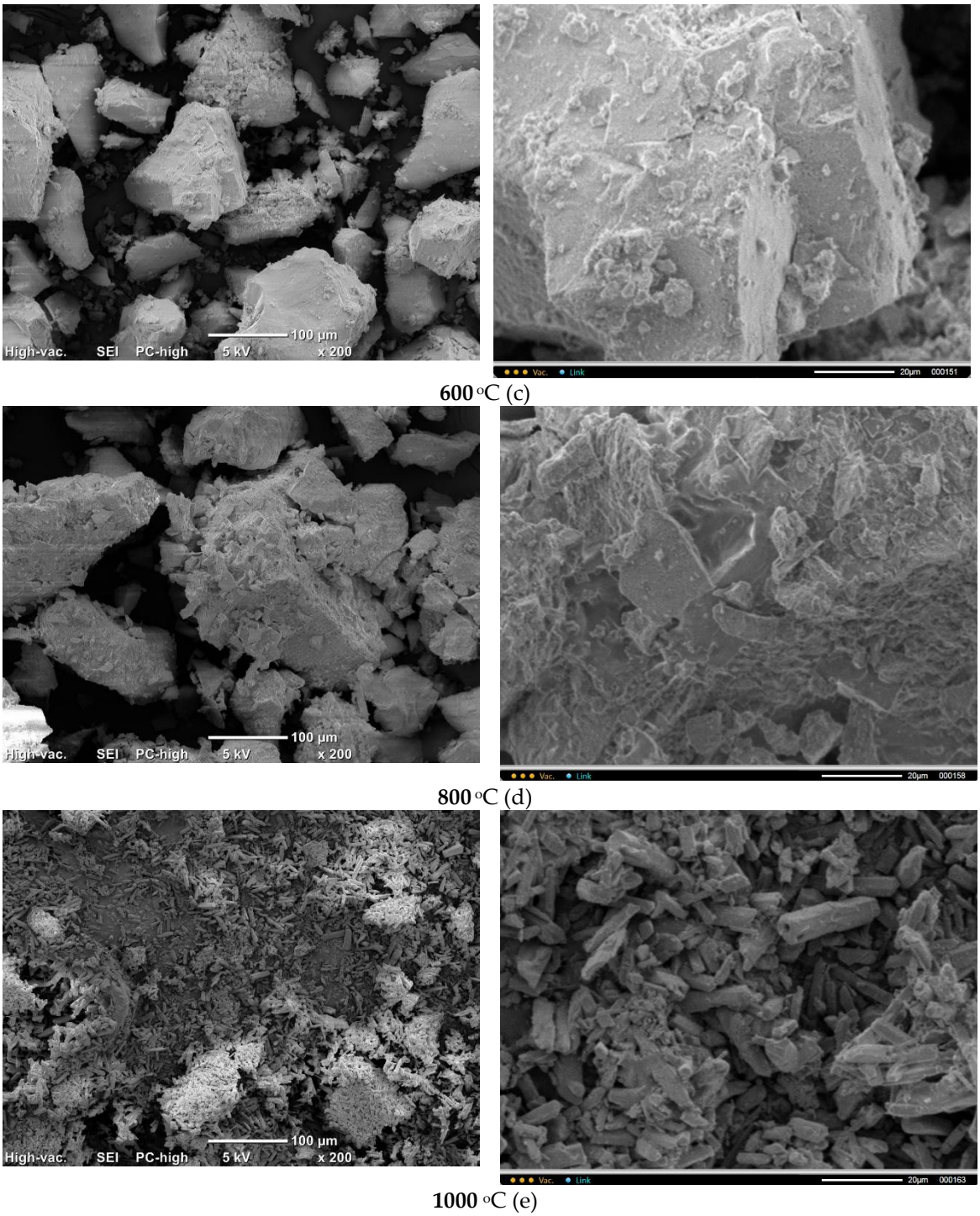

Figure 12. Micrographs of **PO4_CO3** powder after heat treatment at various temperatures: 200 (a), 400 (b), 600 (c), 800 (d), 1000 (e).

Figure 13 shows the FTIR spectroscopy data for **PO4_CO3** powder after synthesis and after heat treatment at 1000 °C. In the spectrum of the **PO4_CO3_1000** powder, there are no peaks that could be attributed to ν(OH), ν(CO_3^{2-}) or π(CO_3^{2-}). The FTIR spectrum for the powder **PO4_CO3_1000** corresponds to the reference data for chlorapatite (SpectraBase Compound ID KKRjtSFM3Pp, https://spectrabase.com/spectrum/KKRjtSFM3Pp).

 doi:10.20944/preprints202508.2229.v1

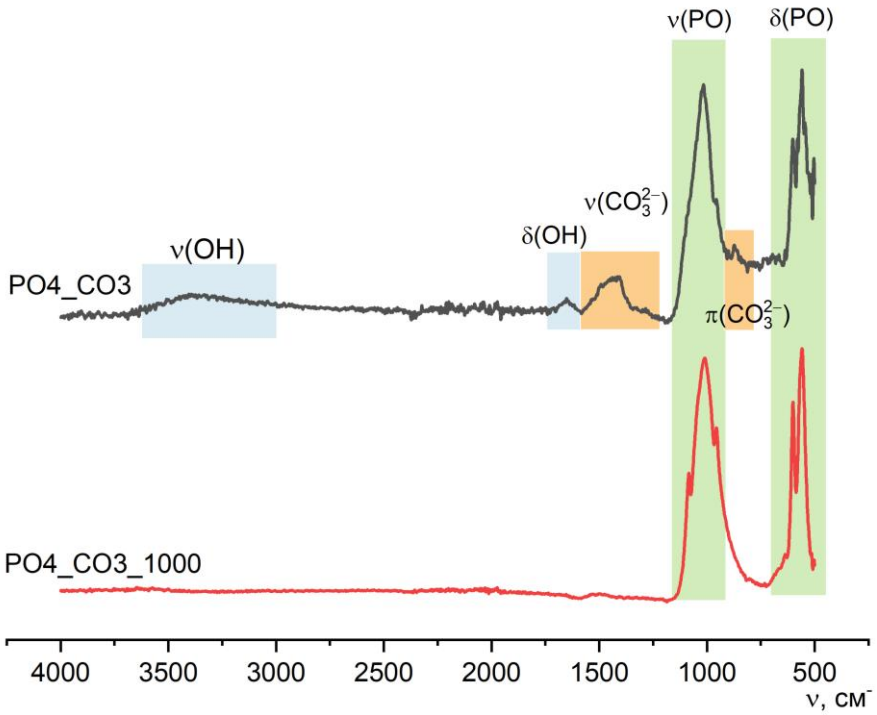

Figure 13. FTIR spectra of **PO4_CO3** powder after synthesis and after heat treatment at 1000 °C.

4. Conclusions

This section is not mandatory but can be added to the manuscript if the discussion is unusually long or complex.

Powders with the phase composition including target products such as brushite $CaHPO_4 \cdot 2H_2O$ and calcium carbonate (calcite) $CaCO_3$, as well as potassium chloride (sylvine) KCl as a reaction by-product, were synthesized from aqueous solutions of calcium chloride $CaCl_2$, potassium hydrophosphate K_2HPO_4 and potassium carbonate K_2CO_3. The interaction of a aqueous mixed anionic solution including HPO_4^{2-} and CO_3^{2-} anions and an aqueous solution of calcium chloride $CaCl_2$ made it possible to obtain a powder that combined weakly crystallized hydroxyapatite and a significant amount (estimated to be up to 30-35% by weight) of potassium chloride (sylvine) KCl in its phase composition. The XRD, SEM, and FTIR data confirmed the possibility of synthesizing chlorapatite $Ca_{10}(PO_4)_6Cl_2$ from this powder via heat treatment at 1000 °C for 2 hours.

After heat treatment of the synthesized powder containing brushite $CaHPO_4 \cdot 2H_2O$ and potassium chloride (sylvine) KCl at 800 and 1000 °C, powders with the phase composition included β-calcium pyrophosphate β-$Ca_2P_2O_7$, β-calcium orthophosphate β-$Ca_3(PO_4)_2$ and potassium calcium pyrophosphate $K_2CaP_2O_7$ was obtained. Heat treatment of calcite $CaCO_3$ powder at 800 °C as it was expected lead to the formation of calcium oxide CaO.

Powders including biocompatible phases such as hydroxyapatite, chlorapatite, brushite, monetite, calcium pyrophosphate, calcium potassium pyrophosphate, tricalcium phosphate, calcite can be used for creation of biocompatible inorganic materials or composite materials with a biocompatible polymer matrix. Potassium chloride (sylvine) KCl present in synthesized powders can act as one of the precursors of biocompatible phases such as chlorapatite or calcium potassium pyrophosphate; or it can act as a removable inorganic porogen.

Author Contributions: Conceptualization, T.V.S.; methodology, T.V.S.; investigation, T.V.S., H.M.N.L., T.B.S., A.M.M., T.V.F., E.A.M., D.M.T., D.O.G., O.V.B. and A.V.K.; resources, T.V.S., T.B.S., D.M.T., O.V.B.; writing—original draft preparation, T.V.S., H.M.N.L.; writing—review and editing, T.V.S.; visualization, T.V.S., H.M.N.L., T.B.S., A.M.M., T.V.F., D.M.T., D.O.G., O.V.B. and A.V.K.; supervision, T.V.S.; project administration, T.V.S.; funding acquisition, T.V.S. All authors have read and agreed to the published version of the manuscript.

 doi:10.20944/preprints202508.2229.v1

Funding: This work was carried out with the support of the State assignment of the Lomonosov Moscow State University, Registration Number No. AAAAA-A21-121011590082-2.

Acknowledgments: This research was carried out using the equipment of the MSU Shared Research Equipment Center "Technologies for obtaining new nanostructured materials and their complex study", and had been purchased by MSU within the framework of the Equipment Renovation Program (National Project "Science"), and within the framework of the MSU Program of Development.

Conflicts of Interest: The authors declare no conflicts of interest.

References

1. Andrianov, N.T.; Balkevich, V.L.; Belyakov, A.V.; Vlasov, A.S.; Guzman, I.Ya.; Lukin, E.S.; ... & Skidan, B.S. Chemical technology of ceramics: textbook. handbook for universities/Edited by I.Ya. Guzman. Moscow: Rif Stroymaterialy LLC, **2012.**-496 p. ISBN 978-5-94026-01966. In Russian
2. Butt Yu.M., Sychev M.M., Timashev V.V. Chemical technology of binder materials [Textbook for universities on spec. "Chemical technology of binding materials"] / Ed. Timasheva V.V. - M. : Higher School, 1980. — 472 p. ill.; 22. In Russian
3. Lee B., Komarneni S., ed. by // Chemical Processing of Ceramics, CRC Press, 2005 Pages 756. eBook ISBN 978-0-42911-963-7, https://doi.org/10.1201/9781420027334.
4. Gerasimov M.D., Latyshev S.S., Bogdanov N.E., Loktionov I.O. Review of constructive solutions in the field of grinding mills // Energy-saving technological complexes and equipment for the production of building materials : An Interuniversity collection of articles / Edited by V.S. Bogdanov. Volume Issue XVII. Belgorod : Belgorod State Technological University named after V.G. Shukhov, **2018,** 132-146. https://www.elibrary.ru/item.asp?id=42997967.
5. Shlyakhtin, O.A., Tretyakov, Y.D. Recent progress in cryochemical synthesis of oxide materials. *J. Mater. Chem.* **1999**, *9*(1), 19-24. https://doi.org/10.1039/A805081C
6. Hiroshi Kageyama, Hiraku Ogino (Eds.). Mixed-anion Compounds. 2024. RSC. Pages 276. ISBN: 978-1-83916-512-2, https://doi.org/10.1039/9781839166372
7. Lukin, E.S.; Makarov, N.A.; Kozlov, A.I.; Popova, N.A.; Anufrieva, E.V.; Vartanyan, M.A.; Kozlov, I.A.; Safina, M.N.; Lemeshev, D.O.; Gorelik E.I. Oxide ceramics of the new generation and areas of application. *Glass Ceram.* **2008**, *65(9)*, 348-352. https://doi.org/10.1007/s10717-009-9085-y
8. Lukin E.S. Modern high-density oxide ceramics with controlled microstructure. Part I. Effect of aggregation of oxide powders on the sintering and microstructure of ceramics. *Refractories* **1996,** *37,* 6–14. https://doi.org/10.1007/BF02230457.
9. Ring T.A. Fundamentals of ceramic powder processing and synthesis. – Elsevier, **1996**. 1st Edition - April 30, 1996, Imprint: Academic Press. eBook ISBN: 9780080532196 https://doi.org/10.1016/B978-0-12-588930-8.X5000-1
10. Safronova, T.V.; Putlyaev, V.I.; Filippov, Y.Y.; Shatalova, T.B.; Fatin D.S. Ceramics Based on Brushite Powder Synthesized from Calcium Nitrate and Disodium and Dipotassium Hydrogen Phosphates. *Inorg. Mater.* **2018**, *54*, 195–207, https://doi.org/10.1134/S0020168518020127
11. Safronova, T.V.; Knot'ko, A.V.; Shatalova, T.B.; Evdokimov, P.V.; Putlyaev, V.I.; Kostin, M.S. Calcium phosphate ceramic based on powder synthesized from a mixed-anionic solution. *Glass Ceram.* **2016**, *73*, 25–31. https://doi.org/10.1007/s10717-016-9819-6.
12. Safronova, T.V.; Putlyaev, V.I.; Filippov, Ya.Yu.; Knot'ko, A.V.; Klimashina, E.S.; Peranidze, K.Kh.; Evdokimov, P.V.; Vladimirova, S.A. Powders synthesized from calcium acetate and mixed-anionic solutions, containing orthophosphate and carbonate ions, for obtaining bioceramic // *Glass Ceram.* **2018,** *75*, 118–123. https://doi.org/10.1007/s10717-018-0040-7.
13. Song, Y.; Hahn, H.H.; Hoffmann, E. The effect of carbonate on the precipitation of calcium phosphate. *Environ. technol.* **2002**, *23(2),* 207-215. https://doi.org/10.1080/09593332508618427.
14. Frank-Kamenetskaya, O.; Kol'tsov, A.; Kuz'mina, M.; Zorina, M.; Poritskaya, L. Ion substitutions and non-stoichiometry of carbonated apatite-(CaOH) synthesised by precipitation and hydrothermal methods. *J. Mol. Struct.* **2011**, *992(1-3)*, 9-18. https://doi.org/10.1016/j.molstruc.2011.02.013.

 doi:10.20944/preprints202508.2229.v1

15. Peranidze, K.; Safronova, T.V.; Filippov, Y.; Kazakova, G.; Shatalova, T.; Rau, J.V. Powders Based on $Ca_2P_2O_7$-$CaCO_3$-H_2O System as Model Objects for the Development of Bioceramics. *Ceramics* **2022**, *5*, 423-434. https://doi.org/10.3390/ceramics5030032
16. Golubchikov, D.; Safronova, T.V.; Nemygina, E.; Shatalova, T.B.; Tikhomirova, I.N.; Roslyakov, I.V.; Khayrutdinova, D.; Platonov, V.; Boytsova, O.; Kaimonov, M.; et al. Powder Synthesized from Aqueous Solution of Calcium Nitrate and Mixed-Anionic Solution of Orthophosphate and Silicate Anions for Bioceramics Production. *Coatings* **2023**, *13*, 374. https://doi.org/10.3390/coatings13020374.
17. Rey, C.; Combes, C.; Drouet, C.; Glimcher, M.J. Bone mineral: update on chemical composition and structure. *Osteoporos. Int.* **2009,** 20, 1013–1021. https://doi.org/10.1007/s00198-009-0860-y.
18. Inorganic Ion Exchange Materials, CRC Press, 2018
19. Ivanets, A.I.; Shashkova, I.L.; Kitikova, N.V.; Radkevich, A.V.; Davydov, Yu.P. Recovery of strontium ions with calcium and magnesium phosphates from aqueous solutions against the background of $CaCl_2$. *Radiochemistry* **2015,** *57(6),* 610-615. https://doi.org/10.1134/S1066362215060089
20. Berlyand A.S., Snyakin A.P., Prokopov A.A. Adsorption capacity of hydroxyapatite for several amino acids and heavy metal ions. *Pharm. Chem. J.* **2012,** *46(5),* 292. https://doi.org/10.1007/s11094-012-0782-4
21. Bystrov, V.S.; Paramonova, E.V.; Filippov, S.V.; Likhachev, I.V.; Bystrova, A.V.; Avakyan, L.A.; Kovrigina, S.A.; Makarova, S.V.; Bulina, N.V. Features of the Structure and Properties of Hydroxypapatite with Various Cationic Substitutions. Proceedings of the International Conference "Mathematical Biology and Bioinformatics". Ed. V.D. Lakhno. Pushchino: IMPB RAS. **2024**, *10,* Paper No. e11. https://doi.org/10.17537/icmbb24.2.
22. Tite, T.; Popa, A.-C.; Balescu, L.M.; Bogdan, I.M.; Pasuk, I.; Ferreira, J.M.F.; Stan, G.E. Cationic Substitutions in Hydroxyapatite: Current Status of the Derived Biofunctional Effects and Their In Vitro Interrogation Methods. *Materials* **2018,** *11,* 2081. https://doi.org/10.3390/ma11112081
23. Jiang, Y.; Yuan, Z.; Huang, J. Substituted hydroxyapatite: a recent development. *Mater. Technol*. **2020,** *35(11-12),* 785-796. https://doi.org/10.1080/10667857.2019.1664096
24. Safronova, T.V., Putlyaev, V.I. Powder systems for calcium phosphate ceramics. *Inorg. Mater.* **2017**, *53*, 17–26 https://doi.org/10.1134/S0020168516130057
25. Kapolos, J.; Koutsoukos, P.G. Formation of calcium phosphates in aqueous solutions in the presence of carbonate ions. *Langmuir.* **1999,** *15(19)*, 6557-6562. https://doi.org/10.1021/la981285k
26. Miron, R.J.; Fujioka-Kobayashi, M.; Pikos, M.A.; Nakamura, T.; Imafuji, T.; Zhang, Y.; Shinohara, Y.; Sculean, A.; Shirakata Y. The development of non-resorbable bone allografts: Biological background and clinical perspectives. *Periodontol. 2000*. **2024,** *94(1),* 161-179. https://doi.org/10.1111/prd.12551
27. He, F.; Zhang, J.; Tian, X.; Wu, S.; Chen, X. A facile magnesium-containing calcium carbonate biomaterial as potential bone graft. *Colloid. Surf., B.* **2015,** *136,* 845-852. https://doi.org/10.1016/j.colsurfb.2015.10.027
28. Huang, Y.; Cao, L.; Parakhonskiy, B.V.; Skirtach, A.G. Hard, Soft, and Hard-and-Soft Drug Delivery Carriers Based on CaCO3 and Alginate Biomaterials: Synthesis, Properties, Pharmaceutical Applications. *Pharmaceutics*. **2022**, *14*, 909. https://doi.org/10.3390/pharmaceutics14050909.
29. Liu, H.; Wen, Z.; Liu, Z.; Yang, Y.; Wang, H.; Xia, X.; ... & Liu, Y. Unlocking the potential of amorphous calcium carbonate: A star ascending in the realm of biomedical application. *Acta Pharm. Sin. B.* **2024**, *14(2),* 602-622. https://doi.org/10.1016/j.apsb.2023.08.027.
30. Min, K.H.; Kim, D.H.; Kim, K.H.; Seo, J.-H.; Pack, S.P. Biomimetic Scaffolds of Calcium-Based Materials for Bone Regeneration. *Biomimetics* **2024,** *9*, 511. https://doi.org/10.3390/biomimetics9090511.
31. Mishchenko O.; Yanovska A.; Kosinov O.; Maksymov D.; Moskalenko R.; Ramanavicius A.; Pogorielo, M. Synthetic Calcium–Phosphate Materials for Bone Grafting. *Polymers* **2023,** *15,* 3822. https://doi.org/10.3390/polym15183822.
32. Tavoni, M.; Dapporto, M.; Tampieri, A.; Sprio, S. Bioactive Calcium Phosphate-Based Composites for Bone Regeneration. *J. Compos. Sci.* **2021,** *5,* 227. https://doi.org/10.3390/jcs5090227.
33. Safronova T.V. Inorganic Materials for Regenerative Medicine. *Inorg. Mater.* **2021,** *57,* 443–474 https://doi.org/10.1134/S002016852105006X.
34. ICDD (2010). PDF-4+ 2010 (Database), edited by Dr. Soorya Kabekkodu, International Centre for Diffraction Data. Newtown Square. PA. USA. http://www.icdd.com/products/pdf2.htm

 doi:10.20944/preprints202508.2229.v1

35. *Nakamoto, K.* Infrared and Raman Spectra of Inorganic and Coordination Compounds, 5th ed.; Wiley: New York, NY, USA, 1986; pp. 156–159.
36. Safronova, T.V.; Sterlikov, G.S.; Kaimonov, M.R.; Shatalova, T.B.; Filippov, Y.Y.; Toshev, O.U.; Roslyakov, I.V.; Kozlov, D.A.; Tikhomirova, I.N.; Akhmedov, M.R. Composite Powders Synthesized from the Water Solutions of Sodium Silicate and Different Calcium Salts (Nitrate, Chloride, and Acetate). *J. Compos. Sci.* **2023**, *7*, 408. https://doi.org/10.3390/jcs7100408.
37. Casciani F., Condrate Sr R.A. The vibrational spectra of brushite, $CaHPO_4 \cdot 2H_2O$. *Spectrosc. Lett.* **1979.** *12(10),* 699-713. doi 10.1080/00387017908069196.
38. Berry, E.E.; Baddiel, C.B. The infra-red spectrum of dicalcium phosphate dihydrate (brushite). *Spectrochim. Acta A-M.* **1967,** *23(7),* 2089-2097. doi 10.1016/0584-8539(67)80097-7.
39. Hirsch, A.; Azuri, I.; Addadi, L.; Weiner, S.; Yang, K.; Curtarolo, S.; Kronik, L. Infrared absorption spectrum of brushite from first principles. *Chem Mater.* **2014,** *26(9),* 2934-2942. https://doi.org/10.1021/cm500650t.
40. Wang, X.; Xu, X.; Ye, Y.; Wang, C.; Liu, D.; Shi, X.; Wang, S.; Zhu, X. In-situ High-Temperature XRD and FTIR for Calcite, Dolomite and Magnesite: Anharmonic Contribution to the Thermodynamic Properties. *J. Earth Sci.* **2019,** *30,* 964–976. https://doi.org/10.1007/s12583-019-1236-7.
41. Bosch Reig, F.; Gimeno Adelantado, J.V.; Moya Moreno, M.C.M. FTIR quantitative analysis of calcium carbonate (calcite) and silica (quartz) mixtures using the constant ratio method. Application to geological samples. *Talanta* **2002**, *58(4),* 811-821. https://doi.org/10.1016/S0039-9140(02)00372-7.
42. Čadež, V.; Šegota, S.; Sondi I.; Lyons, D.M.; Saha, P.; Saha, N.; Sikirić, M.D. Calcium phosphate and calcium carbonate mineralization of bioinspired hydrogels based on β-chitin isolated from biomineral of the common cuttlefish (Sepia officinalis, L.). *J. Polym. Res.* **2018,** *25,* 226. https://doi.org/10.1007/s10965-018-1626-z.
43. Hossain, M.S.; Ahmed, S. FTIR spectrum analysis to predict the crystalline and amorphous phases of hydroxyapatite: a comparison of vibrational motion to reflection. *RSC adv.* **2023**, *13(21),* 14625-14630. https://doi.org/10.1039/D3RA02580B.
44. Lee IH., Lee JA., Lee JH.; Heo, YW; Kim, JJ. Effects of pH and reaction temperature on hydroxyapatite powders synthesized by precipitation. *J. Korean Ceram. Soc.* **2020,** *57,* 56–64. https://doi.org/10.1007/s43207-019-00004-0.
45. Fleet, M.E.; Liu, X. Carbonate apatite type A synthesized at high pressure: new space group (P3) and orientation of channel carbonate ion. *J. Solid State Chem.,* **2003,** *174(2),* 412-417. https://doi.org/10.1016/S0022-4596(03)00281-0.
46. Shiehpour, M.; Solgi, S.; Tafreshi, M.J.; Ghamsari, M.S. ZnO-doped KCl single crystal with enhanced UV emission lines. *Appl. Phys. A* **2019,** *125,* 531 https://doi.org/10.1007/s00339-019-2846-8.
47. Chruszcz-Lipsk,a K.; Zelek-Pogudz, S.; Solecka, U.; Solecki, M.L.; Szostak, E.; Zborowsk,i K.K.; Zając, M. Use of the Far Infrared Spectroscopy for NaCl and KCl Minerals Characterization—A Case Study of Halides from Kłodawa in Poland. *Minerals* **2022,** *12,* 1561. https://doi.org/10.3390/min12121561
48. Toshima, T.; Hamai, R.; Tafu, M.; Takemura, Y.; Fujita, S.; Chohji, T.; Tanda, S.; Li, S.; Qin, G.W. Morphology control of brushite prepared by aqueous solution synthesis. *J. Asian Ceram. Soc.* **2014,** *2(1),* 52-56. https://doi.org/10.1016/j.jascer.2014.01.004.
49. Niu, Y.Q., Liu, J.H., Aymonier, C.; Fermani, S.; Kralj, D.; Falini, G.; Zhou, C.H. Calcium carbonate: controlled synthesis, surface functionalization, and nanostructured materials. *Chem. Soc. Rev.* **2022,** *51(18),* 7883-7943. https://doi.org/10.1039/D1CS00519G.
50. Dosen, A.; Giese, R.F. Thermal decomposition of brushite, $CaHPO_4 \cdot 2H_2O$ to monetite $CaHPO_4$ and the formation of an amorphous phase. *Am. Mineral.* **2011,** *96(2-3),* 368-373. https://doi.org/10.2138/am.2011.3544
51. Safronova, T.; Kuznetsov, A.; Korneychuk, S.; Putlyaev, V.; Shekhirev, M. Calcium phosphate powders synthesized from solutions with $[Ca^{2+}]/[PO_4^{3-}]$=1 for bioresorbable ceramics. *Open Chem.* **2009,** *7(2),* P. 184-191. https://doi.org/10.2478/s11532-009-0016-0.
52. Babou-Kammoe, R.; Hamoudi, S.; Larachi, F.; Belkacemi, K. Synthesis of $CaCO_3$ nanoparticles by controlled precipitation of saturated carbonate and calcium nitrate aqueous solutions. *Can. J. Chem. Eng.* **2012,** *90(1),* 26-33. https://doi.org/10.1002/CJCE.20673.

 doi:10.20944/preprints202508.2229.v1

53. Rabinovich V.A., Khavin Z.Ya. A short chemical reference book. Leningrad.: Chemistry, **1978,** 392 p. in Russian.
54. Zhou, D.; Dong, J.; Si, Y.; Zhu, F.; Li, J. Melting Curve of Potassium Chloride from in situ Ionic Conduction Measurements. *Minerals* **2020,** *10,* 250. https://doi.org/10.3390/min10030250.
55. Cavalcante L.d.A.; Ribeiro L.S.; Takeno M.L.; Aum P.T.P.; Aum Y.K.P.G.; Andrade J.C.S. Chlorapatite Derived from Fish Scales. *Materials* **2020,** *13,* 1129. https://doi.org/10.3390/ma13051129